


Accelerating discovery, enabling scientists
Discover the benefits of using spectral flow cytometry for high-parameter, high-throughput cell analysis



SONY
Download Tech Note



Plasmacytoid Dendritic Cells Promote Host Defense against Acute Pneumovirus Infection via the TLR7 –MyD88-Dependent Signaling Pathway

This information is current as of August 9, 2022.

Sophia Davidson, Gerard Kaiko, Zhixuan Loh, Amit Lalwani, Vivian Zhang, Kirsten Spann, Shen Yun Foo, Nicole Hansbro, Satoshi Uematsu, Shizuo Akira, Klaus I. Matthaei, Helene F. Rosenberg, Paul S. Foster and Simon Phipps

J Immunol 2011; 186:5938-5948; Prepublished online 11 April 2011;
doi: 10.4049/jimmunol.1002635
<http://www.jimmunol.org/content/186/10/5938>

Supplementary Material <http://www.jimmunol.org/content/suppl/2011/04/11/jimmunol.1002635.DC1>

References This article **cites 59 articles**, 24 of which you can access for free at:
<http://www.jimmunol.org/content/186/10/5938.full#ref-list-1>

Why *The JI*? Submit online.

- **Rapid Reviews! 30 days*** from submission to initial decision
- **No Triage!** Every submission reviewed by practicing scientists
- **Fast Publication!** 4 weeks from acceptance to publication

**average*

Subscription Information about subscribing to *The Journal of Immunology* is online at:
<http://jimmunol.org/subscription>

Permissions Submit copyright permission requests at:
<http://www.aai.org/About/Publications/JI/copyright.html>

Email Alerts Receive free email-alerts when new articles cite this article. Sign up at:
<http://jimmunol.org/alerts>

The Journal of Immunology is published twice each month by
The American Association of Immunologists, Inc.,
1451 Rockville Pike, Suite 650, Rockville, MD 20852
All rights reserved.
Print ISSN: 0022-1767 Online ISSN: 1550-6606.



Plasmacytoid Dendritic Cells Promote Host Defense against Acute Pneumovirus Infection via the TLR7–MyD88-Dependent Signaling Pathway

Sophia Davidson,^{*,†} Gerard Kaiko,^{*,†} Zhixuan Loh,^{‡,§} Amit Lalwani,^{‡,§} Vivian Zhang,^{‡,§} Kirsten Spann,[¶] Shen Yun Foo,^{*,†} Nicole Hansbro,^{*,†} Satoshi Uematsu,^{||} Shizuo Akira,^{||} Klaus I. Matthaei,^{#,**} Helene F. Rosenberg,^{††} Paul S. Foster,^{*,†} and Simon Phipps^{‡,§}

Human respiratory syncytial virus (RSV) is the leading cause of lower respiratory tract infection in infants. In human infants, plasmacytoid dendritic cells (pDC) are recruited to the nasal compartment during infection and initiate host defense through the secretion of type I IFN, IL-12, and IL-6. However, RSV-infected pDC are refractory to TLR7-mediated activation. In this study, we used the rodent-specific pathogen, pneumonia virus of mice (PVM), to determine the contribution of pDC and TLR7 signaling to the development of the innate inflammatory and early adaptive immune response. In wild-type, but not TLR7- or MyD88-deficient mice, PVM inoculation led to a marked infiltration of pDC and increased expression of type I, II, and III IFNs. The delayed induction of IFNs in the absence of TLR7 or MyD88 was associated with a diminished innate inflammatory response and augmented virus recovery from lung tissue. In the absence of TLR7, PVM-specific CD8⁺ T cell cytokine production was abrogated. The adoptive transfer of TLR7-sufficient, but not TLR7-deficient pDC to TLR7 gene-deleted mice recapitulated the antiviral responses observed in wild-type mice and promoted virus clearance. In summary, TLR7-mediated signaling by pDC is required for appropriate innate responses to acute pneumovirus infection. It is conceivable that as-yet-unidentified defects in the TLR7 signaling pathway may be associated with elevated levels of RSV-associated morbidity and mortality among otherwise healthy human infants. *The Journal of Immunology*, 2011, 186: 5938–5948.

Respiratory syncytial virus (RSV) is an enveloped, negative-sense ssRNA virus of the family *Paramyxoviridae*, genus *Pneumovirus*. RSV infects approximately two-thirds of all infants in the first year of life and is the leading cause of hospitalization for respiratory tract illnesses (1, 2). Whereas most RSV infections are self limited, severe RSV

bronchiolitis is characterized by pulmonary granulocytic infiltrates, and occlusion of the bronchioles can develop as a result of edema, sloughing of necrotic epithelia from small airways, and increased secretion of mucus (3). Recently, the importance of innate pattern recognition receptors (PRRs) in sensing signature motifs of invading pathogens and in initiating the appropriate innate and adaptive immune response has been realized (4, 5). Dendritic cells (DC) located within the airway mucosa sample foreign molecules and sense viral nucleic acids through the activation of TLRs, the retinoic acid-inducible gene (RIG)-I-like helicase receptor (RLR), and/or nucleotide-binding domain-like receptor (NLR) systems (6–10). Plasmacytoid DC (pDC) were originally described as IFN-producing cells that preferentially use TLR7 and TLR9 to recognize RNA and DNA viruses, respectively. In so doing, these cells initiate an antiviral state and protective immunity through the release of preformed type I IFNs (11–13). Although significant increases in pDC numbers have been detected in nasal wash samples obtained from infants hospitalized with acute RSV infection (14), functional studies performed *in vitro* have revealed that clinical isolates of RSV can infect human pDC and abolish TLR7-mediated production of type I IFN (14, 15). This finding suggests that RSV-induced attenuation of the innate immune response could be among the factors, leading to the development of bronchiolitis and/or incomplete immunity. Despite this, the role of TLR7 in the generation of host defense against pneumovirus infection remains to be determined.

TLR7 is expressed in the endosome and can therefore detect virions following engulfment by endocytosis (i.e., prior to cellular infection) (16, 17). Interestingly, Lee et al. (18) demonstrated that actively replicating, infectious vesicular stomatitis virus promoted a more substantial type I IFN response via TLR7 than was achieved with inactivated, nonreplicating virus. Moreover, human

^{*}Centre for Asthma and Respiratory Diseases, University of Newcastle, New South Wales 2300, Australia; [†]Hunter Medical Research Institute, University of Newcastle, New South Wales 2300, Australia; [‡]School of Biomedical Sciences, University of Queensland, Queensland 4072, Australia; [§]Australian Infectious Diseases Research Centre, University of Queensland, Queensland 4072, Australia; [¶]Sir Albert Sakzewski Virus Research Centre, University of Queensland, Queensland 4029, Australia; ^{||}Laboratory of Host Defense, World Premier International Immunology Frontier Research Center, Osaka University, Osaka 565-0871, Japan; [#]Stem Cell and Gene Targeting Laboratory, John Curtin School of Medical Research, Australian National University, Australian Capital Territory 0200, Australia; ^{**}Stem Cell Unit, Department of Anatomy, College of Medicine and King Khalid University Hospital, King Saud University, Riyadh 11461, Kingdom of Saudi Arabia; and ^{††}National Institute of Allergy and Infectious Diseases, National Institutes of Health, Bethesda, MD 20892

Received for publication August 5, 2010. Accepted for publication March 10, 2011.

This work was supported by a National Health and Medical Research Council of Australia Project grant (to S.P. and P.S.F.) and National Institute of Allergy and Infectious Diseases Division of Intramural Research funding (Z01-AI000943 to H.F.R.). S.P. was a recipient of an Australian Lung Foundation/Boehringer Ingelheim Chronic Airflow Limitation Research Fellowship from 2006 to 2007.

Address correspondence and reprint requests to Dr. Simon Phipps, School of Biomedical Sciences and Australian Infectious Diseases Research Centre, University of Queensland, St. Lucia, QLD 4072, Australia. E-mail address: s.phipps@uq.edu.au

The online version of this article contains supplemental material.

Abbreviations used in this article: DC, dendritic cells; dpi, days postinfection; HPRT, hypoxanthine phosphoribosyltransferase; hRSV, human respiratory syncytial virus; IRF, IFN regulatory factor; NLR, nucleotide-binding domain-like receptor; pDC, plasmacytoid DCs; PRR, pattern recognition receptor; PVM, pneumonia virus of mice; qRT-PCR, quantitative RT-PCR; RIG, retinoic acid-inducible gene; RLR, RIG-I-like helicase receptor; RSV, respiratory syncytial virus; SH, Src homology; WT, wild-type.

RSV induces the release of type I IFN from human pDC in a replication-dependent manner (19). It is clear from these findings that the nature of the infectious pathogen and its ability to replicate in vivo may have substantial impact on the findings obtained. As such, we elected not to use human RSV (hRSV), which replicates poorly in mice. Our study used pneumonia virus of mice (PVM), a rodent-specific pneumovirus pathogen that undergoes robust replication in response to a minimal virion inoculation and models the more severe forms of infantile RSV disease in inbred strains of mice (20, 21). Our study examined the unique contributions of pDC, of the pathogen-sensing receptor, TLR7, and its cognate intracellular adaptor molecule MyD88, in early innate immune recognition and the development of host defense to pneumovirus infection in vivo.

Materials and Methods

Animals and PVM inoculation

All mice were backcrossed to BALB/c for 10 generations and housed at the University of Newcastle specific pathogen-free facility. All experiments were approved by the University of Newcastle Animal Care and Ethics Committee. Stocks of PVM (J3666 strain) were maintained, as described previously (22). Isoflurane-anesthetized mice were inoculated intranasally with 5 PFU PVM in a volume of 10 μ l at 7 d of age. Vehicle (DMEM containing 10% FCS)-inoculated mice served as controls.

Flow cytometry

Leukocytes in the left lung lobe were enumerated by flow cytometry, as described previously (23). Briefly, lung cells were mashed through a cell strainer, and RBCs were lysed with ammonium chloride. Cells were seeded into a U-bottom 96-well plate at 10^6 /well, and preincubated with anti-Fc γ R1/II (Fc block) in PBS/2% FCS medium prior to a 20-min incubation with one or more of the following fluorochrome-labeled Abs (BD Biosciences, unless otherwise stated): FITC- and PE-B220 (RA3-6B2); PerCP-conjugated Gr-1 (RB6-8C5); FITC-conjugated CD3 (145-2C11); allophycocyanin-conjugated CD4 (RM4-5); PerCP-conjugated CD8a (clone 53-6.7); allophycocyanin-conjugated Sca-1 (eBioscience); FITC-conjugated CD11c (clone HL3); PE-conjugated CD49b (clone DX5); PerCP-conjugated CD11b (clone M1/70); and allophycocyanin-conjugated Siglec-H (eBioscience; clone eBio440c). After three washes in PBS/2% FCS medium, cells were resuspended in PBS/formalin (0.5% v/v) and analyzed using a BD CANTO within 3 d.

Quantification of lung gene and protein expression

mRNA was quantified, as described previously (24). Briefly, the left lung lobe was harvested into RNA later (Ambion) and left at 4°C overnight prior to storage at -80°C. The remaining lung lobes, with the exception of the large left lobe (used to measure inflammatory cells), were harvested into 1 ml radioimmunoprecipitation assay buffer (Sigma-Aldrich) and stored at -80°C. RNA was isolated and cDNA transcribed using random primers and Moloney murine leukemia virus reverse transcriptase. The real-time PCR was performed with an ABI 7700 Sequence Detector System (Applied Biosystems, Scoresby, Australia). Expression of a housekeeping gene (hypoxanthine phosphoribosyltransferase [HPRT]) was also determined against plasmid controls to generate a standard curve. Gene expression was normalized against the expression of the housekeeping gene, which was not altered by the treatment, and expressed as fold change compared with vehicle-inoculated wild-type (WT) mice. Primer sequences used were as follows: *IFN- α 4* forward, 5'-ACCAACAGATCCAGAAGGCTCAAG-3' and reverse, 5'-AGTCTTCC-TGGGTCAGAGGAGGTT-3'; *IFN- β* forward, 5'-AGAGTTACACTGCC-TTTGCCATCC-3' and reverse, 5'-CCACGTCAATCTTCTCTTGTCTT-3'; *IFN- λ 2* (IL-28B) forward, 5'-TTGAGAAGGACATGAGGTGACGTT-3' and reverse, 5'-CTCTGCTGTGGCCTGAAGCTGT-3'; *IFN- γ* forward, 5'-TCTTGAAAGACAATCAGGCCATCA-3' and reverse, 5'-GAATC-AGCAGCGACTCCTTTTCC-3'; *IFN regulatory factor (IRF)7* forward, 5'-CTTAGCCGGGAGCTTGGATCTACT-3' and reverse, 5'-CCCTTG-TACATGATGGTCACATCC-3'; *CCL3* forward, 5'-CCTCTGTACCTG-CTCAACA-3' and reverse, 5'-GATGAATTGGCGTGGAAATC-3'; *RIG-I* forward, 5'-ACAAACCACAACCTGTTCTTGACA-3' and reverse, 5'-TGGCGCAGAAATATCTTGTCTTCT-3'; *Mx-1* forward, 5'-GACTCT-CATTGACCTGCCTGGAAT-3' and reverse, 5'-TTACGAAGGCAGTT-TGGACCATCT-3'; *NOD2* forward, 5'-GCCAGTACGAGTGTGAGGA-

GATCA-3' and reverse, 5'-CAGCTCCAAGATGTTCTCCGTGTA-3'; *NLRP3* forward, 5'-GATTGACTTCAATGGCGAGGAGAA-3' and reverse, 5'-AACCTGCTTCTACATGTCTGTCTG-3'; *PVM* Src homology (SH) forward, 5'-GCCTGCATCAACACAGATGTGT-3' and reverse, 5'-GCCTGATGTGGCAGTGTCT-3'; *HPRT* forward, 5'-AGGCCAGACT-TTGTGGATTGAA-3' and reverse, 5'-CAACTGCGCTCATCTTA-GGCTTT-3'.

For analysis of cytokine/chemokine protein expression, the right lung lobes were collected and the tissue homogenized in radioimmunoprecipitation assay buffer using a tissue tearer (Diantree Scientific, Tasmania, Australia). After 10-min incubation on ice, samples were centrifuged at 13,000 rpm for 10 min at 4°C to remove cellular debris. CCL3 (R&D Systems, Gympie, Australia), IL-12p40 (eBioscience), IL-6 (eBioscience), TNF- α (eBioscience), or IFN- γ (BD Biosciences) was measured by ELISA, according to the manufacturer's instructions.

Immunohistochemistry

Lung biopsies from WT and TLR7 gene-deleted mice were processed, and immunohistochemistry was performed, as described previously (25). In brief, sections were permeabilized with saponin/PBS (0.1% w/v) buffer for 30 min, and treated with 10% normal goat serum to reduce nonspecific binding prior to overnight incubation with rabbit anti-TLR7 (Abcam; 10 μ g/ml) or rabbit antiphosphorylated IRF7 (Cell Signaling Technology; 1/50). After three wash steps, alkaline phosphatase-conjugated goat anti-rabbit (Sigma-Aldrich) was incubated at 1/200 dilution. Positive cells stained red after development with Fast Red (Sigma-Aldrich). Cells were counterstained with Harris's hematoxylin (DakoCytomation) and mounted in glycerol (DakoCytomation).

In vivo depletion of pDC

A total of 1.6 mg/kg body weight of functional grade anti-CD317 Ab (BST-2, PDCA-1; eBioscience) was injected into the peritoneum on days 5 and 6 of life.

Generation of pDC from bone marrow

pDC were derived from bone marrow cells of WT and TLR7 gene-deleted mice cultured in 100 ng/ml Flt3-L (a generous gift from Amgen), as described previously (26). On days 3 and 6 of culture, half the media was replenished with Flt3-L-supplemented RPMI 1640.

In vitro infection of pDC with PVM and intracellular IFN- α staining

After a 10-d culture with Flt3-L, unfractionated bone marrow cells were removed from culture flasks, washed, and seeded into 96-well plates at 10^6 /well and incubated at 37°C for 2 h with PVM at a multiplicity of infection of 0.1 before the addition of brefeldin A (5 mg/ml; Sigma-Aldrich). Cells were cultured for an additional 5 h prior to treatment with anti-Fc γ R1/II (Fc block), and then labeled with fluorescence-labeled Abs against B220, CD11c, and Siglec-H. Following fixation and permeabilization, cells were incubated with rat anti-IFN- α at 10 μ g/ml (HyCult Biotechnology; HM1001) for 30 min at 4°C (27). After three wash steps, cells were incubated with a FITC-conjugated rabbit anti-rat Ab (1:500 dilution; Sigma-Aldrich).

Adoptive transfer of purified pDC

On day 10 of culture, bone marrow cells from WT and TLR7 gene-deleted mice were counted and incubated for 30 min on ice with anti-B220-DM beads (BD Biosciences) at a ratio of 2×10^5 cells/ μ l beads. pDC were positively selected using an iMagnet (BD Biosciences) and found to be >95% pure based on Siglec-H and CD11c^{low} expression analyzed by flow cytometry. pDC were resuspended at 25×10^6 cells/ml, and 0.5×10^6 pDC were administered both intranasally and via injection to the peritoneum of TLR7 gene-deleted mice. All mice were inoculated intranasally with 5 PFU PVM 2 h later.

Draining lymph node cell culture and measurement of T cell cytokine production

Draining lymph nodes were removed, and cells were dissociated by applying gentle pressure with a syringe plunger over a cell strainer. RBCs were depleted by ammonium chloride lysis. Cells were resuspended in complete HBSS (HEPES, sodium pyruvate, L-glutamine, 10% v/v FCS, penicillin and streptomycin, 2-ME), seeded into a flat-bottom 96-well plate at 0.3×10^6 /well, and stimulated with P261-270 peptide (28) (CYLTDRARI, Biomolecular Resource Facility, Australian National University) at 20 μ g/

ml or diluent (complete RPMI 1640). After a 3-d incubation, cell-free supernatants were collected and stored at -80°C prior to IFN- γ (BD Biosciences) and TNF (eBioscience) detection by ELISA.

Statistical analysis

Data presented are the means \pm SEM. Data sets were analyzed by Student *t* test, except for the time courses, which were analyzed by ANOVA and Bonferroni post hoc test, and Fig. 5A, in which the Mann-Whitney *U* test was employed. The software package GraphPad Prism 3.01 (GraphPad Software, San Diego, CA) was used for all data analysis and preparation of graphs.

Results

The absence of TLR7 and MyD88 delays the onset of clinical symptoms and viral clearance

Virus detection may occur via a number of innate sensors, including TLRs, RLRs, and NLRs. To determine whether the TLR7 pathway is required for the clearance of the PVM virus pathogen, WT, TLR7 gene-deleted, and MyD88 gene-deleted mice were inoculated at 7 d of age, and virus recovery was measured by quantitative PCR detection assay targeting the PVM SH gene, as described previously (29). Virus titers were elevated at 5 and 7 d postinfection (dpi) in both TLR7- and MyD88 gene-deleted mice as compared with WT mice (Fig. 1A). To assess the impact of this finding on morbidity, mice were weighed daily. PVM-infected WT mice exhibited blunted weight gain from as early as 2 dpi, and diverged significantly from vehicle-inoculated WT mice beginning at 4 dpi (Fig. 1B). In contrast, PVM infection had no impact on weight gain among the 7-d-old TLR7- and MyD88 gene-deleted mice until 7 dpi, when a sudden weight loss (11% of maximum body weight) was observed over the course of 24 h (Fig. 1C, 1D). Of note, the organization of the airway epithelium in the TLR7- and MyD88 gene-deleted mice was disturbed, as evidenced by epithelial cell sloughing and denudation of the basement membrane. The presentation of clinical symptoms followed a similar pattern to weight loss, with WT mice presenting earlier, but with less severe symptoms, including reduced movement and piloerection, than mice deficient in either TLR7 or MyD88 (data not shown). However, in some experiments, a few of the TLR7- and MyD88-deficient mice died between the ages of 5 and 10 dpi.

PVM-induced lung inflammation requires the expression of TLR7 and MyD88

The failure to mount an inflammatory response is often associated with the absence of weight loss (30). To compare the cellular inflammatory responses in lung tissue of PVM-infected WT, TLR7-, and MyD88 gene-deleted mice, mechanically dispersed lung cells were labeled with fluorochrome-conjugated Abs and phenotyped by flow cytometry. In WT mice, infiltrates of neutrophils and NK cells were elevated at 5 dpi and increased further at 7 dpi (Fig. 2A, 2B). In contrast, in the absence of TLR7 and MyD88, no NK cells and only few neutrophils (in TLR7 $^{-/-}$ mice only) were detected at these time points. The NK cell and neutrophil chemoattractant, CCL3, can be expressed by the respiratory epithelium in response to pneumovirus infection in adult WT mice (31), although it is noteworthy that pDC are also a rich source of CCL3 (32, 33). In neonatal mice, we observed elevated CCL3 transcripts within 1 d of PVM inoculation in WT, but not TLR7- or MyD88 gene-deleted mice (data not shown). Immunoreactive CCL3 was detected in whole-lung homogenates at 5 and 7 dpi in WT, but not TLR7- or MyD88 gene-deleted mice, consistent with the observed pattern of neutrophil and NK cell recruitment (Fig. 2C).

pDC recruitment and IFN response are absent in TLR7- and MyD88-deficient mice

Through its cognate receptor CCR5, CCL3 can promote the migration of pDC from the blood to sites of infection (34). In WT mice, inoculation with PVM led to a rapid infiltration of pDC (Siglec-H $^{+}$, CD11c low , B220 $^{+}$) into the lung within 24 h (Fig. 3A, Supplemental Fig. 1). pDC remained elevated until 5 dpi and waned thereafter. By contrast, elevation of pDC numbers was not detected in lungs of TLR7- or MyD88-deficient mice. At 5 dpi, $>80\%$ of WT pDC from PVM-infected mice were positive for MHC class II, an increase from 40% at baseline; no such response was observed in the absence of TLR7 or MyD88 (Fig. 3B). In contrast to pDC, classical DC (CD11c high CD11b high MHC class II high) were not elevated in WT mice following inoculation with PVM. Of note, however, classical DC were greater in TLR7-deficient mice at 7 dpi (data not shown). pDC constitutively

FIGURE 1. The absence of TLR7–MyD88 signaling delays weight loss, clinical symptoms, and virus recovery. Open symbols/scale bars represent vehicle-inoculated mice; closed symbols/scale bars, PVM-inoculated mice. WT mice are represented by circles; TLR7 $^{-/-}$ mice by triangles; and MyD88 $^{-/-}$ mice by diamonds. A, Virus recovery (copies of PVM SH gene per 10^7 copies HPRT) in the lungs of WT, TLR7 $^{-/-}$, and MyD88 $^{-/-}$ mice was measured by quantitative RT-PCR (qRT-PCR) at 1, 3, 5, and 7 dpi. WT (B), TLR7 $^{-/-}$ (C), and MyD88 $^{-/-}$ (D) mice were weighed at 7 d of age immediately prior to inoculation (day 0) with vehicle or PVM. Mice were weighed every 24 h thereafter until euthanasia, and weight was expressed relative to day 0. Data are mean \pm SEM, 4–13 mice in each group. **p* < 0.05, ***p* < 0.01, ****p* < 0.001.

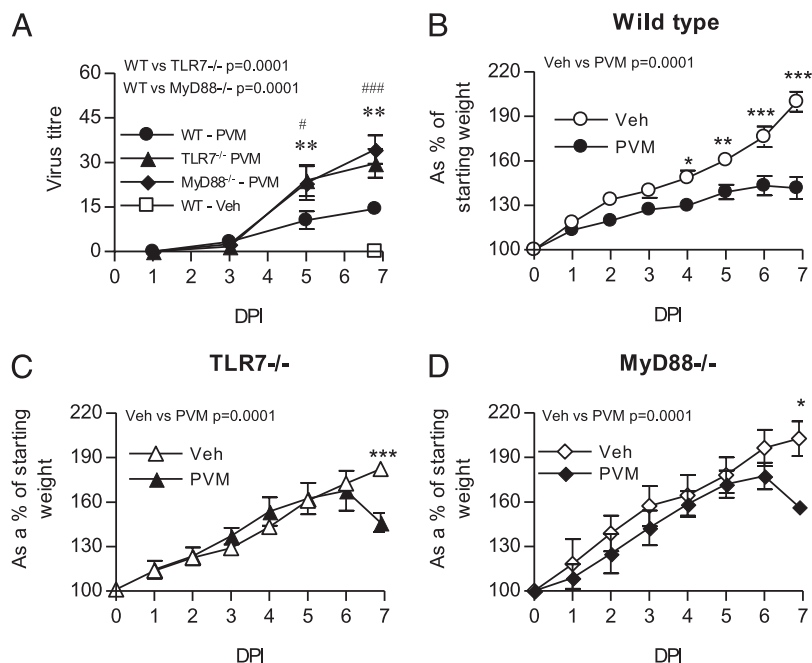
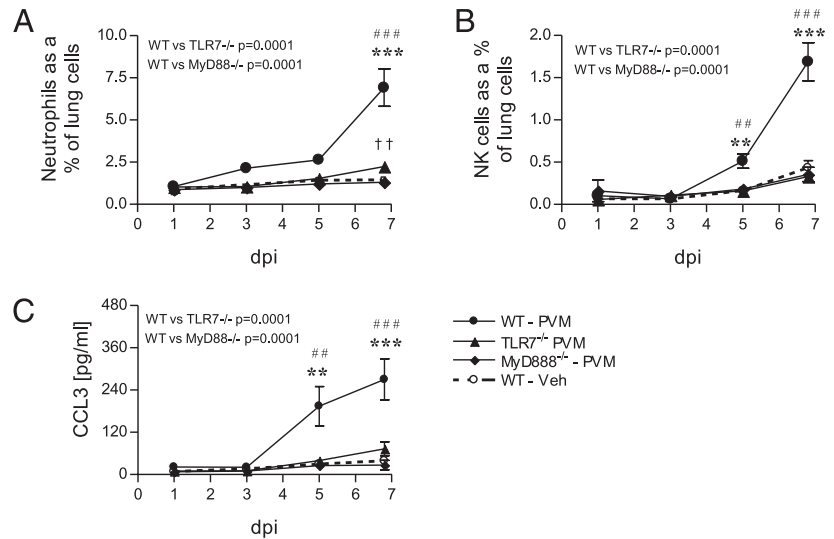


FIGURE 2. PVM inoculation of WT, but not TLR7- or MyD88-deficient neonatal (7-d-old) BALB/c mice induces an innate inflammatory response. Open symbols represent vehicle-inoculated mice; closed symbols, PVM-inoculated mice. WT mice are represented by circles; TLR7^{-/-} mice by triangles; and MyD88^{-/-} mice by diamonds. The left lung lobe was mechanically dispersed, and FSC^{low}Gr-1^{high} CD11b⁺ CD11c⁻ neutrophils (A) and CD3⁻CD49b⁺ NK cells (B) were identified by flow cytometry. C, CCL3 protein expression in right lung lobe homogenates was measured by ELISA. Data are mean \pm SEM, 4–16 mice in each group. * $p < 0.05$, ** $p < 0.01$, *** $p < 0.001$. *WT compared with TLR7-deficient mice, #WT compared with MyD88-deficient mice.



express type I IFNs and IRF7 (35), an important transcription factor activated downstream of TLR and RLR signaling. We detected augmented levels of IFN- α 4 and IFN- β transcripts in the lung in WT, but not TLR7- or MyD88-deficient mice at 5 dpi (Fig. 3C; all data normalized against WT vehicle controls). Likewise, IRF7 was upregulated in WT, but not TLR7- or MyD88-deficient mice (Fig. 3C). Similar findings were obtained for the type III IFN, IFN- λ 2 (IL-28A; Fig. 3C), and the IFN-stimulated gene Mx-1 (data not shown). Collectively, these data suggest that the early induction of IFNs and IFN-stimulatory genes in response to inoculation with PVM was dependent on the TLR7–MyD88 signaling pathway.

Innate cytokine responses are attenuated in the absence of TLR7 or MyD88

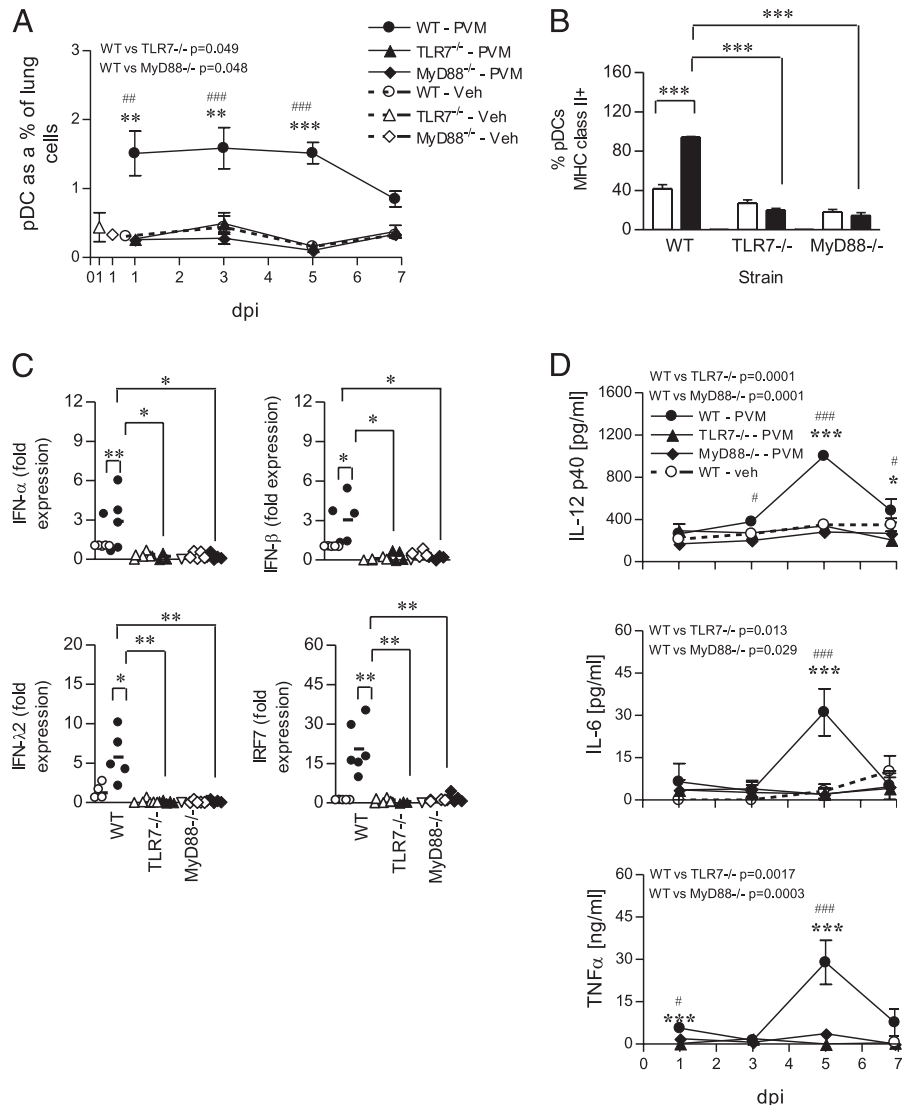
In addition to IFNs, activated pDC are a rich source of proinflammatory cytokines, such as IL-12, IL-6, and TNF, which promote the development of cell-mediated and humoral immunity (27, 36). IL-12p40 was detected in lung homogenates of PVM-infected WT mice at 3 dpi (Fig. 3D), peaked at 5 dpi, and then waned, but remained elevated at 7 dpi. In contrast, IL-12p40 expression remained at constant low levels throughout in PVM-infected TLR7- and MyD88 gene-deleted mice. Similarly, IL-6 and TNF expression peaked at 5 dpi and returned to baseline levels by 7 dpi, and were likewise dependent on TLR7–MyD88 signaling (Fig. 3D). Further studies will be required to confirm the cellular source of these cytokines.

T cell activation and the IFN- γ response require TLR7 and MyD88

In adult mice, PVM infection is associated with pulmonary T cell activation (37). To determine whether the T cells in the lungs of neonatal mice were activated in response to PVM, we measured surface expression of Sca-1, an Ag that responds positively to stimulation with IFN- α (38). At 7 dpi, the fraction of Sca-1⁺CD4⁺ T cells detected from WT mice inoculated with PVM had increased as compared with those from mice inoculated with vehicle control (Fig. 4A). In contrast, the fraction of CD4⁺Sca-1⁺ T cells was unaltered following PVM inoculation of TLR7- or MyD88 gene-deleted mice (Fig. 4A). Analysis of CD8⁺ T cells revealed an identical profile; augmented expression of Sca-1 in response to PVM was likewise dependent on TLR7 and MyD88 (Fig. 4B). IFN- γ is produced by activated NK cells, Th1 cells, and cytotoxic CD8⁺ T cells. In response to infection, augmented expression of

transcripts encoding IFN- γ was observed at 5 dpi (Fig. 4C). Further increases were observed by 7 dpi, most likely as a result of the increasing numbers of NK cells (Fig. 2B). In contrast, IFN- γ transcripts and protein expression were significantly lower in both TLR7- and MyD88-deficient mice as compared with WT mice (Fig. 4C, 4D). However, of note, the concentration of immunoreactive IFN- γ in infected mice was significantly greater than vehicle-inoculated mice in both TLR7- and MyD88-deficient mice at 7 dpi (Fig. 4D). Moreover, there was a significant increase in the expression of IFN- γ protein in the TLR7-, but not MyD88-deficient mice at 7 dpi, indicating that another receptor family that operates via MyD88 (conceivably an IL-1 family member such as IL-18) may also contribute to the induction of IFN- γ . Using tetramer technology, Claassen et al. (28) have previously demonstrated that 11% of CD8⁺ T cells in the lungs of PVM-infected adult mice are specific for the P261 peptide. To address whether the absence of TLR7 affected the production of IFN- γ by PVM-specific CD8⁺ T cells, mediastinal lymph node cells were isolated at 10 dpi and stimulated with the P261 peptide. Although the degree of lymph node hyperplasia did not differ between WT and TLR7 gene-deleted mice (data not shown), CD8⁺ T cells as a fraction of mediastinal lymph node cells were significantly reduced in the absence of TLR7 (Fig. 5A). Correspondingly, in WT mice, P261 peptide stimulation induced the production of both IFN- γ and TNF- α , but this response was significantly attenuated in the absence of TLR7 (Fig. 5B). Intriguingly, the fraction of lung CD8⁺ T cells positive for Sca-1 was now ~40% in both the WT and TLR7-deficient mice, even in the absence of pDC recruitment in the TLR7-deficient mice (data not shown). Together with the elevated neutrophilia (Fig. 2C) and IFN- γ expression (Fig. 4D) at 7 dpi, these data suggest that a delayed type I and type II IFN response occurs in the absence of TLR7. Therefore, we examined the lungs of TLR7-sufficient and TLR7-deficient mice at 7 and 10 dpi for IFN- α 4, Mx-1, CCL3, and transcripts of other PRR known to participate in antiviral immunity, namely RIG-1, NOD2, and NLRP3. Consistent with our findings at 5 dpi (see Fig. 3C), IFN- α 4 expression remained low at 7 dpi in the absence of TLR7. However, there was a dramatic burst of IFN- α transcription at 10 dpi, and this superseded the levels observed in WT mice (Fig. 5C). Consistent with the late IFN- α response, TLR7-deficient mice presented with a delayed increase in the expression of the IFN-stimulatory genes CCL3 and Mx-1 (Fig. 5C). These data suggested that in the absence of TLR7, another PRR can be activated to induce an IFN response albeit with markedly slower kinetics.

FIGURE 3. pDC recruitment and PVM-induced IFN and proinflammatory cytokine production require TLR7–MyD88. Open symbols/scale bars represent vehicle-inoculated mice; closed symbols/scale bars, PVM-inoculated mice. WT mice are represented by circles; TLR7^{-/-} mice by triangles; and MyD88^{-/-} mice by diamonds. The key to symbols is shown in A and is applicable to C and D. A, The left lung lobe was mechanically dispersed, and pDC (Siglec-H⁺, CD11c^{low}, B220⁺) expressed as a percentage of lung cells. pDC from vehicle-inoculated TLR7- and MyD88-deficient mice are shown at day 1 only for clarity. B, Percentage of MHC class II-positive pDC in the lung at 5 dpi in response to vehicle or PVM. C, qRT-PCR analysis of IFN- α 4, IFN- β , IFN- λ 2, and IRF-7 mRNA expression in whole lung from WT, TLR7^{-/-}, and MyD88^{-/-} mice (normalized to lungs from vehicle-inoculated WT mice) at 5 dpi. D, Right lung homogenates were analyzed at 1, 3, 5, and 7 dpi for IL-12p40, IL-6, and TNF- α protein expression by ELISA. Data are represented as mean \pm SEM, four to eight mice in each group, or shown as individual mice. * p < 0.05, ** p < 0.01, *** p < 0.001. #WT compared with TLR7-deficient mice, #WT compared with MyD88-deficient mice.



Of the PRRs, all three were elevated in WT mice, whereas only RIG-I showed a >2-fold increase in the absence of TLR7 (Fig. 5C).

TLR7-sufficient, but not TLR7-deficient pDC recapitulate host defense and decrease viral load

In order to elucidate further the requirement for TLR7 in pDC recognition of PVM, we cultured FLT3-L bone marrow-derived TLR7-sufficient (TLR7^{+/+}) and TLR7-deficient (TLR7^{-/-}) pDC in vitro. Cultured cells were challenged with PVM and stained for IFN- α production by intracellular cytokine staining by flow cytometry. Challenge with PVM augmented the expression of IFN- α in TLR7-sufficient (Fig. 6A, upper panels), but not TLR7-deficient (lower panels) pDC (B220⁺Siglec-H⁺ cells), as summarized in Fig. 6B.

TLR7-sufficient, but not TLR7-deficient pDC recapitulate host defense and decrease viral load

Although PVM-induced IFN- α expression in pDC was TLR7 dependent, it remained possible that non-pDC may contribute to the TLR7-dependent antiviral responses observed in vivo. To determine the cellular distribution of TLR7 expression in the lungs of naive neonatal mice, we employed immunohistochemistry. In addition to leukocytes residing or circulating through the tissue,

TLR7 immunoreactivity was present in the majority of airway epithelial cells (Fig. 7A, left panels). In contrast, no immunoreactivity was seen in both TLR7-deficient mice (Fig. 7A, right panels) and isotype-matched controls. Uniquely, pDC constitutively express IRF7, whereas IRF7 is transcriptionally regulated by type I IFNs in nonhematopoietic cells (35, 39). Thus, engagement of TLR7 in the absence of IRF7 would not prevent IFN-I production. Because IRF7 is phosphorylated in response to TLR7 stimulation, we used a phospho-IRF7-specific Ab and performed immunohistochemistry on tissue biopsies obtained at 1 dpi. Critically, we observed that all of the immunoreactive cells were in the parenchymal tissue, consistent with the localization of pDC in the lung shown by others (40). In contrast, airway epithelial cells of both large and small airways were negative for phospho-IRF7 at 1 dpi (Fig. 7B). Critically, when we depleted pDC with anti-CD317 prior to inoculation, the number of phospho-IRF7-positive cells at 1 dpi was markedly reduced.

To further address whether the phenotype of TLR7-deficient mice was primarily due to the absence of TLR7 on pDC, we generated highly pure pDC populations from FLT3L-cultured bone marrow of TLR7-sufficient and TLR7-deficient mice and adoptively transferred these cells via the intranasal and i.p. routes to TLR7-deficient mice 2 h prior to inoculation with PVM. The transfer of TLR7-sufficient, but not TLR7-deficient pDC led to the

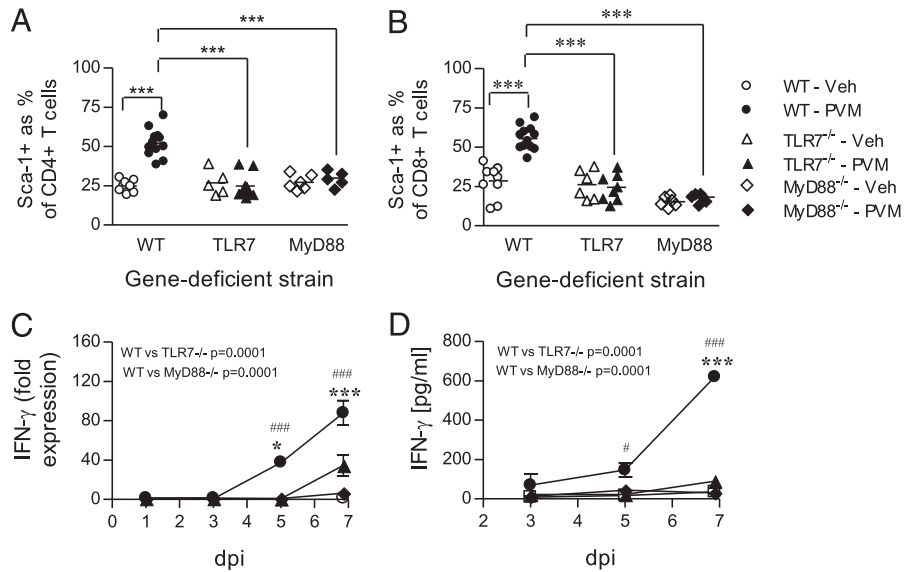


FIGURE 4. Activation of the TLR7–MyD88 pathway is essential for T cell infiltration, activation, and production of IFN- γ . Open symbols/scale bars represent vehicle inoculated; closed symbols/scale bars, PVM inoculated. WT mice are represented by circles; TLR7^{-/-} by triangles; and MyD88^{-/-} by diamonds. *A* and *B*, The percentage of CD4⁺ (*A*) and CD8⁺ (*B*) T cells expressing stem cell Ag-1 (Sca-1, also known as LY6A, a surrogate marker of IFN activation) in the lungs of WT, TLR7^{-/-}, and MyD88^{-/-} mice was quantitated by flow cytometry at 7 dpi. *C* and *D*, IFN- γ gene and protein expression was measured in whole lung by qRT-PCR (*C*) and ELISA (*D*) at 1, 3, 5, and 7 dpi. Data are mean \pm SEM, five mice in each group. **p* < 0.05, ***p* < 0.01, ****p* < 0.001. Data in *A* and *B* were compared by unpaired *t* test and in *C* and *D* by ANOVA and Bonferroni post hoc test. **p* < 0.05, ****p* < 0.001. #WT compared with TLR7-deficient mice, #WT compared with MyD88-deficient mice.

development of an innate inflammatory response at 7 dpi, characterized by recruitment of neutrophils and NK cells and expression of the chemokine CCL3 (Fig. 8*A–C*) to an extent that was comparable to that observed in WT mice (Fig. 2). Production of TNF (Fig. 8*D*) was also observed following transfer of TLR7-sufficient pDC, although interestingly, this had no impact on expression of IL-6 (data not shown). Similarly, TLR7-sufficient, but not TLR7-deficient pDC resulted in augmented Sca-1 expression on both CD4⁺ and CD8⁺ T cells (Fig. 8*E*), suggesting that the activation of TLR7 on pDC is also necessary for the production of

type I IFN. Consistent with our earlier findings, the induction of the cellular inflammatory response in the TLR7-deficient mice as a result of the reconstitution with TLR7-sufficient pDC led to stunted growth as measured by body weight, whereas transfer of TLR7-deficient pDC led to a similar pattern of weight gain to that observed in TLR7-deficient mice (Fig. 8*F* versus Fig. 1*B*, 1*C*). Likewise, the induction of an early inflammatory response following the transfer of TLR7-sufficient pDC was associated with significantly diminished virus recovery when compared with mice that received TLR7-deficient pDC (Fig. 8*G*).

FIGURE 5. PVM-specific CD8⁺ T cell responses and the innate IFN response are delayed in the absence of TLR7. WT (circles) and TLR7-deficient (triangles) mice were inoculated with PVM (closed) or vehicle (open) and sacrificed 10 d later. *A*, The percentage of lymph node cells that were CD3⁺CD8⁺ T cells at 10 dpi. *B*, Mediastinal lymph nodes were harvested, seeded at 0.3×10^6 /well, and stimulated with the PVM-specific peptide (P261) or media alone. After a 3-d culture, cell-free supernatants were quantified for IFN- γ and TNF- α protein expression. *C*, IFN- α 4, CCL3, Mx-1, RIG-I, NOD2, and NLRP3 gene expression in whole-lung extracts was measured by qRT-PCR. Data are mean \pm SEM, five to six mice in each group. Data in *B* were compared by a two-tailed Mann–Whitney, and in *A* and *C* by unpaired *t* test. **p* < 0.05, ***p* < 0.01.

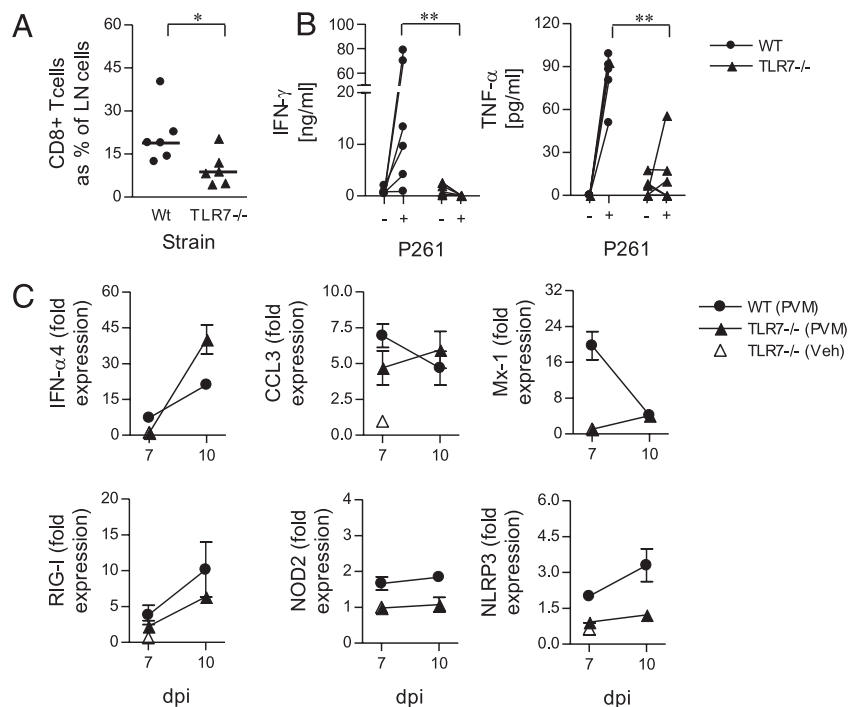
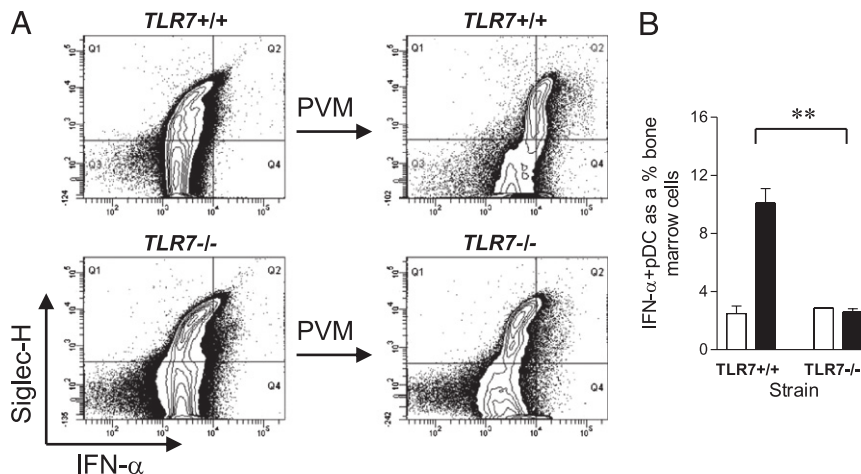


FIGURE 6. PVM-induced upregulation of IFN- α expression by bone marrow-derived pDC requires TLR7. *A*, Bone marrow cells were harvested and cultured in Flt3-L to generate a pDC-rich cell population (~20%). After a 10-d culture, cells were cultured overnight with PVM at a multiplicity of infection of 1 in the presence of brefeldin A. IFN- α was detected by intracellular cytokine staining and localized to Siglec-H⁺, B220⁺ cells. *B*, The percentage of Siglec-H⁺IFN- α ⁺ cells as a fraction of total Flt3-L-treated WT and TLR7^{-/-} bone marrow cells cultured with or without PVM. Data are mean \pm SEM, three to four mice in each group. ** $p < 0.01$.



Discussion

RSV is a primary etiologic agent of bronchiolitis in infants and is associated with significant morbidity in this population. In this

study, we employed the natural rodent pneumovirus pathogen, PVM, to model the more severe forms of RSV disease in mice and to investigate the role of TLR7 in promoting host defense. Using neonatal mice to reflect the more typical age of initial RSV infection in humans, we demonstrated that the absence of TLR7 or its intracellular adaptor protein MyD88 led to a diminished innate immune response and to significantly augmented virus recovery from lung tissue of infected mice. The adoptive transfer of TLR7-sufficient, but not TLR7-deficient pDC restored the innate inflammatory response and resulted in diminished virus recovery, suggesting that TLR7-mediated recognition of PVM by pDC constitutes a critical pathway in the initiation of a timely and appropriate immune response to acute pneumovirus infection in the neonatal period.

Elevated numbers of pDC have been detected in nasal washings of infants with severe RSV infections (14). Consistent with this, we observed recruitment of pDC into the lungs of PVM-infected WT mice as early as 24 h after inoculation. This response was not observed in TLR7- or MyD88 gene-deleted mice, which suggests that the TLR7-MyD88 pathway is engaged early on during the course of infection to mediate the early recruitment of pDC. Viral recognition may occur via the activation of resident leukocytes known to express TLR7 [e.g., pDC, conventional DC, monocytes, B cells (17)], or following detection by airway epithelial cells, which we identify in this study as being highly immunoreactive for TLR7. Based on the literature, pDC are uniquely placed to perform this task because they constitutively express high levels of the IRF7 (particularly in contrast to nonhematopoietic cells) (35, 39, 41), a necessary transcription factor for TLR7-induced transcription of type I IFN. Thus, non-pDC may be largely incompetent and unable to execute TLR7-mediated signals in the initial phase of the host response. In an attempt to discern the relative contribution of hematopoietic cells versus non-hematopoietic cells to TLR7-mediated recognition in the immediate phase of infection, we obtained lung tissue sections at 1 dpi and probed for phosphorylated IRF7 by immunohistochemistry. Immunoreactive cells were found in the parenchyma only, and not in the airway epithelium, indicating that the TLR7-IRF7 cascade is activated primarily in leukocytes at this time. Because the depletion of pDC reduced the number of phospho-IRF7-immunoreactive cells to baseline levels, it is likely that pDC are among the first cells to respond to the virus, even though pDC constitute only ~0.5% of all lung cells. We speculate that the upregulation of IRF7 transcripts 5 dpi enables the epithelium to generate type I IFN in response to TLR7 engagement. However, because the activation of TLR7 can induce a non-IRF7-dependent signaling cascade, we cannot exclude the possibility that the epithelium is

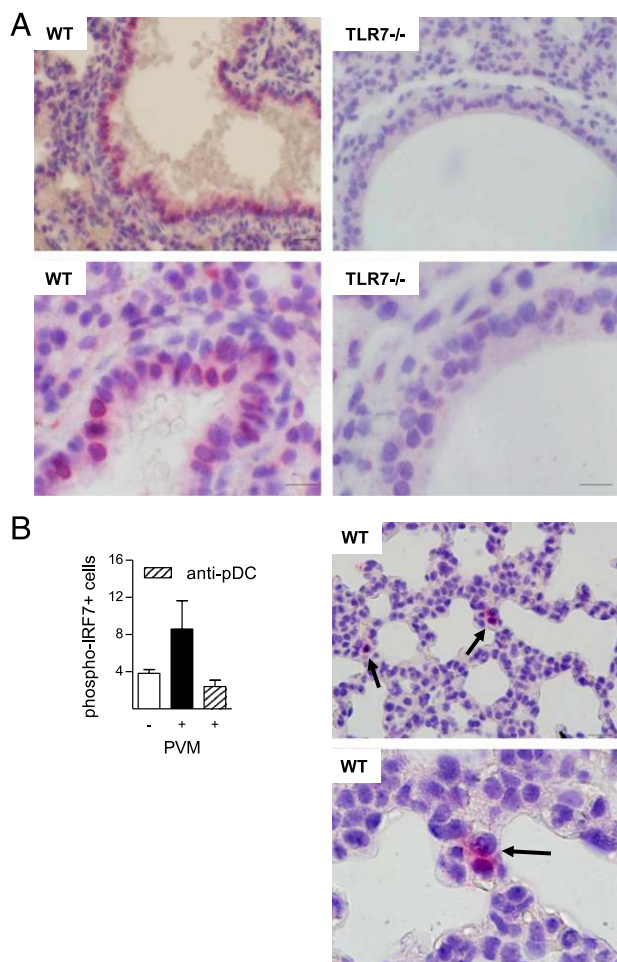
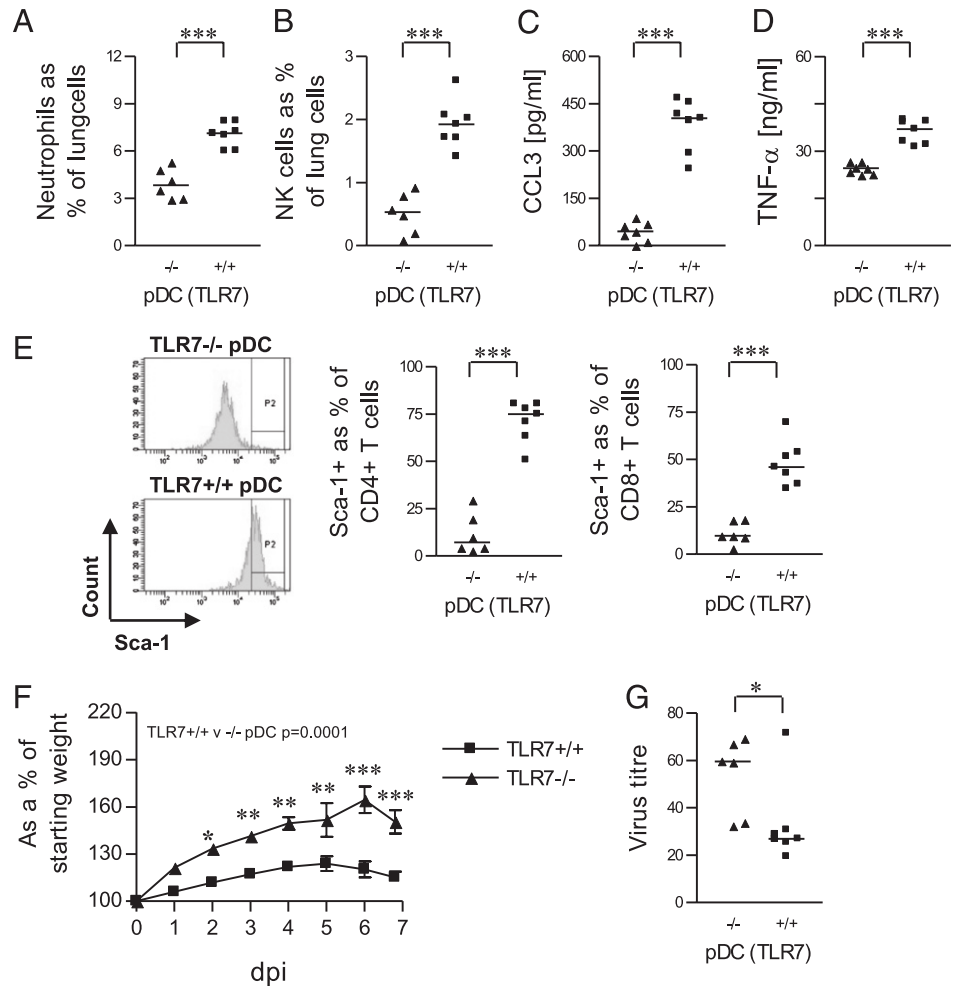


FIGURE 7. TLR7, but not phosphorylated IRF7, is widely distributed. *A*, Lung biopsies from naive neonatal WT (left panels) and TLR7-deficient (right panels) mice were probed for TLR7. The substrate used was fast red and the counter-stain was haematoxylin. Top panels, Scale bar, 20 μ m (original magnification $\times 400$); bottom panels, scale bars, 10 μ m (original magnification $\times 1000$). *B*, Enumeration of phosphorylated IRF7-immunoreactive cells in WT mice at 1 dpi following inoculation with vehicle or PVM \pm anti-pDC Ab, and photomicrograph demonstrating phosphorylated IRF7-immunoreactive cells in PVM-inoculated WT mice. Top panel, Scale bar, 20 μ m (original magnification $\times 400$); bottom panel, scale bar, 10 μ m (original magnification $\times 1000$).

FIGURE 8. Reconstitution of TLR7^{-/-} mice with TLR7^{+/+}, but not TLR7^{-/-} BM-derived pDC recapitulates host defense and accelerates viral clearance. Purified Flt3-L-expanded pDC from TLR7^{+/+} and TLR7^{-/-} bone marrow cells were adoptively transferred to TLR7^{-/-} recipients. Mice were inoculated with PVM 2 h later, and end points were measured at 7 dpi (A, B). The left lung lobe was mechanically dispersed, and A, neutrophils (FSC^{low}Gr-1^{high}CD11b⁺CD11c⁻) and NK cells (CD3⁻CD49b⁺) were identified by flow cytometry. C and D, CCL3 and TNF- α protein expression in right lung lobe homogenates was measured by ELISA. E, Representative histogram of lung CD3⁺CD4⁺Sca-1⁺ T cells following transfer of TLR7^{-/-} (top panel) and TLR7^{+/+} (bottom panel) pDC to TLR7^{-/-} mice. Graphs represent the percentage of CD3⁺CD4⁺ and CD3⁺CD8⁺ T cells expressing Sca-1, as detected by flow cytometry. F, Recipient TLR7^{-/-} mice were weighed at 7 d of age immediately prior to inoculation with PVM (day 0). Mice were weighed every 24 h thereafter until euthanasia, and weight was expressed relative to day 0. G, Virus recovery in the lungs was measured by qRT-PCR. **p* < 0.05, ***p* < 0.01, ****p* < 0.001.



an active participant in the initial phase of infection also. Future studies will need to address the specific contribution of the epithelium to viral recognition and the prevention of viral dissemination.

In an illuminating study, Colonna and colleagues (42) generated pDC-diphtheria toxin receptor knockin mice to inducibly deplete pDC. The findings from this study and those in which Ab-mediated depletion of pDC has been performed suggest that pDC provide the immediate source of type I IFN. Consistent with this paradigm, we observed that the transfer of TLR7-sufficient, but not TLR7-deficient pDC enabled the recapitulation of the innate response at the same magnitude as that observed in infected WT mice. Future studies using the pDC-diphtheria toxin receptor knockin mice or bone marrow chimeras (in adult mice) will further clarify the contribution of pDC; however, based on our findings, we postulate that in response to PVM, pDC mediate the immediate antiviral innate response.

CCL3 has been detected in airway secretions from RSV-infected infants (43), and CCL3/CCR1 is crucial for neutrophil recruitment in response to PVM (44). In this study, we detected production of CCL3 that was temporally associated with the infiltration of neutrophils and NK cells to the lung of WT mice; expression of CCL3 as well as neutrophil and NK cell recruitment were eliminated in both TLR7- and MyD88 gene-deleted mice. Although we did not specifically examine the cellular source of the CCL3, others have demonstrated that pDC, but not myeloid DC, can generate an array of chemokines, including CCL3 (32, 33, 45). In addition, pDC may indirectly induce the expression of CCL3

through the release of IFN- α (46), although we have shown previously that PVM-induced upregulation of CCL3 occurs in the absence of IFN- α receptors (22). In stark contrast to WT mice in which blunted weight growth was observed as early as 4 dpi, in both TLR7- and MyD88-deficient mice the absence of an inflammatory response led to normal weight gain. However, the absence of an early TLR7/MyD88-mediated innate inflammatory (NK cell and neutrophil) response and CTL activation led to increased virus recovery at 5 and 7 dpi. Of note, both the TLR7- and MyD88-deficient, but not WT mice, exhibited >10% loss in body weight, but at 7 dpi. The adoptive transfer of TLR7-sufficient (but not deficient) pDC to TLR7-deficient mice led to the restoration of CCL3 (and TNF- α) production and associated neutrophilia to recapitulate the attenuated weight growth observed in infected WT mice. In contrast, mice that received TLR7-deficient pDC presented a late fall in body weight. Our data suggest that TLR7-mediated activation of pDC promotes the early innate inflammatory response that underlies the early and mild pathophysiological symptoms of disease. The delayed and heightened morbidity that was evident in the absence of TLR7 may suggest that pDC are protective, although longer-term studies will be needed to validate this.

In some studies, some of the TLR7-deficient and MyD88-deficient mice died at 4–7 dpi in the absence of any clinical symptoms, and prior to the onset of cellular inflammation. For ethical reasons, we were unable to perform a definitive LD₅₀ study; however, these findings consolidate the notion that the absence of TLR7 is not beneficial (as might be inferred from the

lack of clinical symptoms at 4 dpi). Intriguingly, emerging clinical data suggest that the absence of NK cells may be related to increasing severity of disease (3, 47–49). Analysis of lung tissue from infants with fatal cases of RSV has revealed a near absence of NK cells and CTLs (48), whereas the bronchial epithelia of these subjects was highly immunoreactive for RSV Ag, indicative of virus replication *in situ*. Future studies will need to address whether alterations in TLR7 expression or function (or related signaling molecules) predispose toward virus-associated bronchiolitis. In addition, it remains to be determined whether the delayed presentation of symptoms observed in the gene-deleted mice occurred as a result of a late, albeit weak innate response in these mice, or whether it was related to increased virus replication and associated cellular damage. However, we did observe that the organization of the airway epithelium of TLR7-deficient mice was significantly perturbed, with evidence of denudation of the basement membrane and epithelial cell sloughing, similar to that seen in clinical autopsy specimens (3). We speculate that whereas the absence of the innate inflammatory response protects against the early presentation of morbidities, the resultant failure to control the virus may either lead to mortality through epithelial dysfunction and airway obstruction by edema, or cause a delayed, but heightened inflammatory response that causes significant morbidity.

Although the focus of this study was the effect of TLR7 deficiency on the innate inflammatory response, we also demonstrated that T cell activation and production of effector cytokines were attenuated in the absence of TLR7, supporting the notion that activation of the innate immune response is critical for the induction of T cell priming. A limitation of this experiment was the absence of a tetramer-based strategy to enumerate absolute numbers of P261-specific T cells; however, it is noteworthy that in the absence of TLR7, the fraction of CD8⁺ T cells in the mediastinal lymph nodes was reduced by 50%, whereas the production of both IFN- γ and TNF was reduced by >95 and >80%, respectively. Consistent with our findings, influenza-specific IFN- γ production from memory CD4⁺, but not CD8⁺ T cells was significantly reduced in mice lacking TLR7 (50). In contrast, lymphocytoid choriomeningitis virus-specific CTL responses were not affected by the absence of TLR7, although in this latter study the CTL response was found to be MyD88 dependent (51). This discrepancy in host response may relate to the host's repertoire of PRR that can recognize any given pathogen as well as the ability of the pathogen to evade detection or subvert immune function (50, 52–54). In our study, it is possible that the attenuated P261 PVM-specific CTL response in TLR7-deficient mice marked a delayed adaptive response as a consequence of the delayed innate response. Alternatively, the secondary PRR system engaged in the absence of TLR7-mediated recognition may be less effective in inducing a robust adaptive response. As such, it will be interesting to determine whether the TLR7–MyD88 pathway is necessary for the development of a protective Ab and memory T cell responses to PVM, as has been shown for influenza virus and RSV (50, 55).

The nature of the alternative PRR system remains unknown. The elevated IFN- γ protein and the upregulation of RIG-I gene expression in TLR7-, but not MyD88-deficient mice implicate a role for another MyD88-dependent Toll–IL-1R family member, such as TLR4 (56) or the IL-1 β R complex. Of note, influenza virus has recently been shown to activate the NLRP3 inflammasome, which catalyzes the formation of biologically active IL-1 β through the activation of caspase-1 (7, 8). In addition to NLRP3, both NOD2 and RIG-I can induce the activation of caspase-1 and have been reported to recognize RSV-derived ssRNA (10, 55). We observed an increase in RIG-I, but not NOD2 or NLRP3 gene expression

from 5 to 10 dpi in TLR7-deficient mice. Other paramyxoviruses (such as RSV, measles, mumps, and Sendai virus) are recognized by RIG-I, and we speculate that the activation of RIG-I (as opposed to MDA-5) may underlie the late IFN response observed in this study. It should also be noted that RIG-I and IRF7 were upregulated in WT mice, consistent with the notion that the early release of type I IFN by pDC bolsters the RLR system to support viral recognition by nonspecialized cells (6, 57). Taken together, the novel findings presented in this work suggest a hierarchy among PRR systems in the recognition of PVM, whereby activation of the TLR7–MyD88 axis in pDC not only establishes the early antiviral state, but also primes other innate sensors such as the RLR and NLR systems. Thus, the strategic targeting of pDC by RSV (15) and/or genetic polymorphisms associated with key genes in the TLR7-signaling pathway (e.g., IRF7) may have significant consequences for the induction of host defense and underlies susceptibility to RSV-induced bronchiolitis and pneumonia.

It is conceivable that the failure to clear the virus increases its dissemination and infectivity of additional cell types that may preferentially employ the alternative PRR. Indeed, our observation that the airway epithelium was damaged in TLR7-deficient, but not TLR7-sufficient mice lends support to this proposition. It is also possible that this PRR is activated as a result of the greater viral burden that occurs in the absence of TLR7. In preliminary experiments, we have observed that inoculation with higher doses of PVM induces markedly higher concentrations of IL-1 β in TLR7-deficient as compared with WT mice (data not shown), suggesting that viral detection may be dose dependent. Our observations have significant ramifications for studies in mice in which sizable inocula (10^5 – 10^7 PFU hRSV per mouse) are used to recover virions at later time points. Other studies that have used gene-deleted mice found that the clearance of hRSV in mice was more dependent on the RLR than the TLR family (55, 58). However, pDC-depleted mice are also characterized by higher viral titres (59, 60). Because pDC are proposed to primarily sense viruses via TLR7 and TLR9, it is difficult to reconcile these findings. Because the TLR7–MyD88 pathway is employed by pDC, whereas the RLR system (and possibly TLR7 pathway) is used by epithelial cells, we speculate that inoculation with high doses of RSV triggers an inflammatory response that is predominantly mediated via activation of RLRs. Our findings emphasize the need to distinguish between virus replication and simple Ag recognition when investigating the molecular and cellular processes that underlie host–pathogen interactions. Thus, as PVM is recognized, infects, and replicates within the host, the natural sequelae of events can be followed, and as a consequence, the temporal hierarchy of innate receptor-mediated recognition and cellular activation can be better delineated.

In summary, our study has focused on a host-specific pneumovirus that initiates severe respiratory disease at physiological inocula in a neonatal mouse model to investigate the mechanisms that underlie the immediate innate responses to pneumovirus infection in human infants. Collectively, our findings underscore a critical role for TLR7 and MyD88 in the early recognition and development of an immediate innate inflammatory response necessary to limit pneumovirus load.

Acknowledgments

We thank Amgen for the generous gift of Flt3-L.

Disclosures

The authors have no financial conflicts of interest.

References

1. Glezen, P., and F. W. Denny. 1973. Epidemiology of acute lower respiratory disease in children. *N. Engl. J. Med.* 288: 498–505.
2. Hall, C. B. 2001. Respiratory syncytial virus and parainfluenza virus. *N. Engl. J. Med.* 344: 1917–1928.
3. Aherne, W., T. Bird, S. D. Court, P. S. Gardner, and J. McQuillin. 1970. Pathological changes in virus infections of the lower respiratory tract in children. *J. Clin. Pathol.* 23: 7–18.
4. Trinchieri, G. 2003. Interleukin-12 and the regulation of innate resistance and adaptive immunity. *Nat. Rev. Immunol.* 3: 133–146.
5. Akira, S., S. Uematsu, and O. Takeuchi. 2006. Pathogen recognition and innate immunity. *Cell* 124: 783–801.
6. Takeuchi, O., and S. Akira. 2008. MDA5/RIG-I and virus recognition. *Curr. Opin. Immunol.* 20: 17–22.
7. Thomas, P. G., P. Dash, J. R. Aldridge, Jr., A. H. Ellebedy, C. Reynolds, A. J. Funk, W. J. Martin, M. Lamkanfi, R. J. Webby, K. L. Boyd, et al. 2009. The intracellular sensor NLRP3 mediates key innate and healing responses to influenza A virus via the regulation of caspase-1. *Immunity* 30: 566–575.
8. Allen, I. C., M. A. Scull, C. B. Moore, E. K. Holl, E. McElvania-TeKippe, D. J. Taxman, E. H. Guthrie, R. J. Pickles, and J. P. Ting. 2009. The NLRP3 inflammasome mediates in vivo innate immunity to influenza A virus through recognition of viral RNA. *Immunity* 30: 556–565.
9. Ichinohe, T., H. K. Lee, Y. Ogura, R. Flavell, and A. Iwasaki. 2009. Inflammasome recognition of influenza virus is essential for adaptive immune responses. *J. Exp. Med.* 206: 79–87.
10. Sabbah, A., T. H. Chang, R. Harnack, V. Frohlich, K. Tominaga, P. H. Dube, Y. Xiang, and S. Bose. 2009. Activation of innate immune antiviral responses by Nod2. *Nat. Immunol.* 10: 1073–1080.
11. Kato, H., S. Sato, M. Yoneyama, M. Yamamoto, S. Uematsu, K. Matsui, T. Tsujimura, K. Takeda, T. Fujita, O. Takeuchi, and S. Akira. 2005. Cell type-specific involvement of RIG-I in antiviral response. *Immunity* 23: 19–28.
12. Sun, Q., L. Sun, H. H. Liu, X. Chen, R. B. Seth, J. Forman, and Z. J. Chen. 2006. The specific and essential role of MAVS in antiviral innate immune responses. *Immunity* 24: 633–642.
13. Ito, T., Y. H. Wang, and Y. J. Liu. 2005. Plasmacytoid dendritic cell precursors/type I interferon-producing cells sense viral infection by Toll-like receptor (TLR) 7 and TLR9. *Springer Semin. Immunopathol.* 26: 221–229.
14. Gill, M. A., A. K. Palucka, T. Barton, F. Ghaffar, H. Jafri, J. Banchereau, and O. Ramilo. 2005. Mobilization of plasmacytoid and myeloid dendritic cells to mucosal sites in children with respiratory syncytial virus and other viral respiratory infections. *J. Infect. Dis.* 191: 1105–1115.
15. Schlender, J., V. Hornung, S. Finke, M. Günther-Biller, S. Marozin, K. Brzózka, S. Moghim, S. Endres, G. Hartmann, and K. K. Conzelmann. 2005. Inhibition of Toll-like receptor 7- and 9-mediated alpha/beta interferon production in human plasmacytoid dendritic cells by respiratory syncytial virus and measles virus. *J. Virol.* 79: 5507–5515.
16. Kawai, T., and S. Akira. 2010. The role of pattern-recognition receptors in innate immunity: update on Toll-like receptors. *Nat. Immunol.* 11: 373–384.
17. Mancuso, G., M. Gambuzza, A. Midiri, C. Biondo, S. Papisergi, S. Akira, G. Teti, and C. Beninati. 2009. Bacterial recognition by TLR7 in the lysosomes of conventional dendritic cells. *Nat. Immunol.* 10: 587–594.
18. Lee, H. K., J. M. Lund, B. Ramanathan, N. Mizushima, and A. Iwasaki. 2007. Autophagy-dependent viral recognition by plasmacytoid dendritic cells. *Science* 315: 1398–1401.
19. Hornung, V., J. Schlender, M. Guenther-Biller, S. Rothenfusser, S. Endres, K. K. Conzelmann, and G. Hartmann. 2004. Replication-dependent potent IFN-alpha induction in human plasmacytoid dendritic cells by a single-stranded RNA virus. *J. Immunol.* 173: 5935–5943.
20. Rosenberg, H. F., C. A. Bonville, A. J. Easton, and J. B. Domachowske. 2005. The pneumonia virus of mice infection model for severe respiratory syncytial virus infection: identifying novel targets for therapeutic intervention. *Pharmacol. Ther.* 105: 1–6.
21. Rosenberg, H. F., and J. B. Domachowske. 2008. Pneumonia virus of mice: severe respiratory infection in a natural host. *Immunol. Lett.* 118: 6–12.
22. Garvey, T. L., K. D. Dyer, J. A. Ellis, C. A. Bonville, B. Foster, C. Prussin, A. J. Easton, J. B. Domachowske, and H. F. Rosenberg. 2005. Inflammatory responses to pneumovirus infection in IFN-alpha beta R gene-deleted mice. *J. Immunol.* 175: 4735–4744.
23. Phipps, S., C. E. Lam, G. E. Kaiko, S. Y. Foo, A. Collison, J. Mattes, J. Barry, S. Davidson, K. Oreo, L. Smith, et al. 2009. Toll/IL-1 signaling is critical for house dust mite-specific helper T cell type 2 and type 17 [corrected] responses. *Am. J. Respir. Crit. Care Med.* 179: 883–893.
24. Phipps, S., N. Hansbro, C. E. Lam, S. Y. Foo, K. I. Matthaei, and P. S. Foster. 2009. Allergic sensitization is enhanced in early life through Toll-like receptor 7 activation. *Clin. Exp. Allergy* 39: 1920–1928.
25. Kaiko, G. E., S. Phipps, P. Angkaskewin, C. Dong, and P. S. Foster. 2010. NK cell deficiency predisposes to viral-induced Th2-type allergic inflammation via epithelial-derived IL-25. *J. Immunol.* 185: 4681–4690.
26. Björck, P. 2001. Isolation and characterization of plasmacytoid dendritic cells from Flt3 ligand and granulocyte-macrophage colony-stimulating factor-treated mice. *Blood* 98: 3520–3526.
27. Diebold, S. S., T. Kaisho, H. Hemmi, S. Akira, and C. Reis e Sousa. 2004. Innate antiviral responses by means of TLR7-mediated recognition of single-stranded RNA. *Science* 303: 1529–1531.
28. Claassen, E. A., G. M. van Bleek, Z. S. Rychnavska, R. J. de Groot, E. J. Hensen, E. J. Tjhaar, W. van Eden, and R. G. van der Most. 2007. Identification of a CD4 T cell epitope in the pneumonia virus of mice glycoprotein and characterization of its role in protective immunity. *Virology* 368: 17–25.
29. Percopo, C. M., Z. Qiu, S. Phipps, P. S. Foster, J. B. Domachowske, and H. F. Rosenberg. 2009. Pulmonary eosinophils and their role in immunopathologic responses to formalin-inactivated pneumonia virus of mice. *J. Immunol.* 183: 604–612.
30. Moyron-Quiroz, J. E., J. Rangel-Moreno, K. Kusser, L. Hartson, F. Sprague, S. Goodrich, D. L. Woodland, F. E. Lund, and T. D. Randall. 2004. Role of inducible bronchus associated lymphoid tissue (iBALT) in respiratory immunity. *Nat. Med.* 10: 927–934.
31. Bonville, C. A., N. J. Bennett, M. Koehnlein, D. M. Haines, J. A. Ellis, A. M. DelVecchio, H. F. Rosenberg, and J. B. Domachowske. 2006. Respiratory dysfunction and proinflammatory chemokines in the pneumonia virus of mice (PVM) model of viral bronchiolitis. *Virology* 349: 87–95.
32. Penna, G., M. Vulcano, A. Roncari, F. Facchetti, S. Sozzani, and L. Adorini. 2002. Cutting edge: differential chemokine production by myeloid and plasmacytoid dendritic cells. *J. Immunol.* 169: 6673–6676.
33. Krug, A., R. Uppaluri, F. Facchetti, B. G. Dörner, K. C. Sheehan, R. D. Schreiber, M. Cella, and M. Colonna. 2002. IFN-producing cells respond to CXCR3 ligands in the presence of CXCL12 and secrete inflammatory chemokines upon activation. *J. Immunol.* 169: 6079–6083.
34. Yoneyama, H., K. Matsuno, Y. Zhang, T. Nishiwaki, M. Kitabatake, S. Ueha, S. Narumi, S. Morikawa, T. Ezaki, B. Lu, et al. 2004. Evidence for recruitment of plasmacytoid dendritic cell precursors to inflamed lymph nodes through high endothelial venules. *Int. Immunol.* 16: 915–928.
35. Honda, K., H. Yanai, H. Negishi, M. Asagiri, M. Sato, T. Mizutani, N. Shimada, Y. Ohba, A. Takaoka, N. Yoshida, and T. Taniguchi. 2005. IRF-7 is the master regulator of type-I interferon-dependent immune responses. *Nature* 434: 772–777.
36. Jago, G., A. K. Palucka, J. P. Blanck, C. Chalouni, V. Pascual, and J. Banchereau. 2003. Plasmacytoid dendritic cells induce plasma cell differentiation through type I interferon and interleukin 6. *Immunity* 19: 225–234.
37. Claassen, E. A., P. A. van der Kant, Z. S. Rychnavska, G. M. van Bleek, A. J. Easton, and R. G. van der Most. 2005. Activation and inactivation of antiviral CD8 T cell responses during murine pneumovirus infection. *J. Immunol.* 175: 6597–6604.
38. Khan, K. D., K. Shuai, G. Lindwall, S. E. Maher, J. E. Darnell, Jr., and A. L. Bothwell. 1993. Induction of the Ly-6A/E gene by interferon alpha/beta and gamma requires a DNA element to which a tyrosine-phosphorylated 91-kDa protein binds. *Proc. Natl. Acad. Sci. USA* 90: 6806–6810.
39. Honda, K., Y. Ohba, H. Yanai, H. Negishi, T. Mizutani, A. Takaoka, C. Taya, and T. Taniguchi. 2005. Spatiotemporal regulation of MyD88-IRF-7 signalling for robust type-I interferon induction. *Nature* 434: 1035–1040.
40. de Heer, H. J., H. Hammad, T. Soullier, D. Hijdra, N. Vos, M. A. Willart, H. C. Hoogsteden, and B. N. Lambrecht. 2004. Essential role of lung plasmacytoid dendritic cells in preventing asthmatic reactions to harmless inhaled antigen. *J. Exp. Med.* 200: 89–98.
41. Barchet, W., M. Cella, B. Odermatt, C. Asselin-Paturel, M. Colonna, and U. Kalinke. 2002. Virus-induced interferon alpha production by a dendritic cell subset in the absence of feedback signaling in vivo. *J. Exp. Med.* 195: 507–516.
42. Swiecki, M., S. Gilfillan, W. Vermi, Y. Wang, and M. Colonna. 2010. Plasmacytoid dendritic cell ablation impacts early interferon responses and antiviral NK and CD8(+) T cell accrual. *Immunity* 33: 955–966.
43. Garofalo, R. P., J. Patti, K. A. Hintz, V. Hill, P. L. Ogra, and R. C. Welliver. 2001. Macrophage inflammatory protein-1alpha (not T helper type 2 cytokines) is associated with severe forms of respiratory syncytial virus bronchiolitis. *J. Infect. Dis.* 184: 393–399.
44. Domachowske, J. B., C. A. Bonville, J. L. Gao, P. M. Murphy, A. J. Easton, and H. F. Rosenberg. 2000. The chemokine macrophage-inflammatory protein-1 alpha and its receptor CCR1 control pulmonary inflammation and antiviral host defense in paramyxovirus infection. *J. Immunol.* 165: 2677–2682.
45. Del Corral, M., M. C. Gauzzi, G. Penna, F. Belardelli, L. Adorini, and S. Gessani. 2005. Human immunodeficiency virus type 1 gp120 and other activation stimuli are highly effective in triggering alpha interferon and CC chemokine production in circulating plasmacytoid but not myeloid dendritic cells. *J. Virol.* 79: 12597–12601.
46. Salazar-Mather, T. P., C. A. Lewis, and C. A. Biron. 2002. Type I interferons regulate inflammatory cell trafficking and macrophage inflammatory protein 1alpha delivery to the liver. *J. Clin. Invest.* 110: 321–330.
47. Welliver, T. P., J. L. Reed, and R. C. Welliver, Sr. 2008. Respiratory syncytial virus and influenza virus infections: observations from tissues of fatal infant cases. *Pediatr. Infect. Dis. J.* 27(Suppl. 10):S92–S96.
48. Welliver, T. P., R. P. Garofalo, Y. Hosakote, K. H. Hintz, L. Avendano, K. Sanchez, L. Velozo, H. Jafri, S. Chavez-Buono, P. L. Ogra, et al. 2007. Severe human lower respiratory tract illness caused by respiratory syncytial virus and influenza virus is characterized by the absence of pulmonary cytotoxic lymphocyte responses. *J. Infect. Dis.* 195: 1126–1136.
49. De Weerd, W., W. N. Twilhaar, and J. L. Kimpen. 1998. T cell subset analysis in peripheral blood of children with RSV bronchiolitis. *Scand. J. Infect. Dis.* 30: 77–80.
50. Koyama, S., K. J. Ishii, H. Kumar, T. Tanimoto, C. Coban, S. Uematsu, T. Kawai, and S. Akira. 2007. Differential role of TLR- and RLR-signaling in the immune responses to influenza A virus infection and vaccination. *J. Immunol.* 179: 4711–4720.
51. Jung, A., H. Kato, Y. Kumagai, H. Kumar, T. Kawai, O. Takeuchi, and S. Akira. 2008. Lymphocytoid choriomeningitis virus activates plasmacytoid den-

- dratic cells and induces a cytotoxic T-cell response via MyD88. *J. Virol.* 82: 196–206.
52. Barchet, W., A. Krug, M. Cella, C. Newby, J. A. Fischer, A. Dzionic, A. Pekosz, and M. Colonna. 2005. Dendritic cells respond to influenza virus through TLR7- and PKR-independent pathways. *Eur. J. Immunol.* 35: 236–242.
 53. Mandl, J. N., A. P. Barry, T. H. Vanderford, N. Kozyr, R. Chavan, S. Klucking, F. J. Barrat, R. L. Coffman, S. I. Staprans, and M. B. Feinberg. 2008. Divergent TLR7 and TLR9 signaling and type I interferon production distinguish pathogenic and nonpathogenic AIDS virus infections. *Nat. Med.* 14: 1077–1087.
 54. Heinze, B., S. Frey, M. Mordstein, A. Schmitt-Gräff, S. Ehl, U. J. Buchholz, P. L. Collins, P. Stäheli, and C. D. Krempf. 2011. Both nonstructural proteins 1 and 2 of pneumonia virus of mice are inhibitors of the interferon type I and III response in vivo. *J. Virol.*
 55. Bhoj, V. G., Q. Sun, E. J. Bhoj, C. Somers, X. Chen, J. P. Torres, A. Mejias, A. M. Gomez, H. Jafri, O. Ramilo, and Z. J. Chen. 2008. MAVS and MyD88 are essential for innate immunity but not cytotoxic T lymphocyte response against respiratory syncytial virus. *Proc. Natl. Acad. Sci. USA* 105: 14046–14051.
 56. Kurt-Jones, E. A., L. Popova, L. Kwinn, L. M. Haynes, L. P. Jones, R. A. Tripp, E. E. Walsh, M. W. Freeman, D. T. Golenbock, L. J. Anderson, and R. W. Finberg. 2000. Pattern recognition receptors TLR4 and CD14 mediate response to respiratory syncytial virus. *Nat. Immunol.* 1: 398–401.
 57. Sato, M., H. Suemori, N. Hata, M. Asagiri, K. Ogasawara, K. Nakao, T. Nakaya, M. Katsuki, S. Noguchi, N. Tanaka, and T. Taniguchi. 2000. Distinct and essential roles of transcription factors IRF-3 and IRF-7 in response to viruses for IFN- α / β gene induction. *Immunity* 13: 539–548.
 58. Rudd, B. D., M. A. Schaller, J. J. Smit, S. L. Kunkel, R. Neupane, L. Kelley, A. A. Berlin, and N. W. Lukacs. 2007. MyD88-mediated instructive signals in dendritic cells regulate pulmonary immune responses during respiratory virus infection. *J. Immunol.* 178: 5820–5827.
 59. Smit, J. J., B. D. Rudd, and N. W. Lukacs. 2006. Plasmacytoid dendritic cells inhibit pulmonary immunopathology and promote clearance of respiratory syncytial virus. *J. Exp. Med.* 203: 1153–1159.
 60. Wang, H., N. Peters, and J. Schwarze. 2006. Plasmacytoid dendritic cells limit viral replication, pulmonary inflammation, and airway hyperresponsiveness in respiratory syncytial virus infection. *J. Immunol.* 177: 6263–6270.